One-way Flow of a Rarefied Gas Induced in a Circular Pipe with a Periodic Temperature Distribution

K. Aoki,* Y. Sone,* S. Takata,* K. Takahashi,* and G. A. Bird†

*Department of Aeronautics and Astronautics, Graduate School of Engineering, Kyoto University, Kyoto 606-8501, Japan
†GAB Consulting, 5 Fiddens Wharf Road, Killara, N.S.W. 2071, Australia

Abstract. The steady behavior of a rarefied gas in a circular pipe with a saw-like temperature distribution increasing and decreasing periodically in the direction of the pipe axis is investigated numerically by means of the direct simulation Monte Carlo method. It is shown that a steady one-way flow is induced in the pipe without the help of a pressure gradient for a wide range of the Knudsen number when a series of ditches is dug periodically in the part of the pipe wall with decreasing (or increasing) temperature. The features of the flow are clarified in detail. It is also shown that the flow has a pumping effect. In particular, some data that give the estimate of the maximum compression ratio attained by a pipe consisting of a large number of periods are presented. The present study is the continuation of the previous study in the case of a two-dimensional channel [Y. Sone *et al.*, Phys. Fluids **8**, 2227 (1996)]. It is found that although the induced one-way flow is stronger for the two-dimensional channel, the pumping effect is stronger for the circular pipe.

INTRODUCTION

In a previous paper [1], the behavior of a rarefied gas in a two-dimensional channel between two plane walls with a periodic temperature distribution was investigated numerically by the direct simulation Monte Carlo (DSMC) method [2,3], and it was shown that a one-way flow is induced in the channel without the help of a pressure gradient for a wide range of the Knudsen number when a series of ditches of a suitable shape is dug periodically on the walls. The features of the flow and its pumping effect were clarified. This flow is of practical importance for the following reason.

As is well known, the usual thermal transpiration (a rarefied gas flow induced in a channel or pipe with a unidirectional temperature gradient; see, e.g., [4–7]) has a pumping effect [4]. That is, if two reservoirs containing a rarefied gas are joined by a channel with a temperature gradient, the gas moves from the reservoir at the cold end to that at the hot end. As a result, a pressure difference arises between the reservoirs, and a steady state in which the thermal transpiration is counterbalanced by the flow due to the pressure gradient is established finally. The pressure difference in this situation is the maximum one maintained by the channel. In order to obtain a larger pressure difference, we should just make the channel longer, keeping the same temperature gradient. However, this fact leads to a practical difficulty that for a long channel we have to impose a huge temperature difference between both ends. In contrast, in the case of the above-mentioned one-way flow caused by a periodic temperature distribution, we can make the channel as long as we wish without any difficulty to obtain a large pressure difference. Therefore, it has a potential applicability as a pump or compressor without any moving part. (See [1,8,9] for the detailed discussions and related references.)

In the present study, we investigate this one-way flow and its pumping effect in the case of a circular pipe which seems to be equally (or even more) important in practical applications. As in [1], the standard DSMC method by Bird [2,3] is employed as the solution method. It should be mentioned here that simple experiments demonstrating this one-way flow clearly were carried out by Sone and coworkers recently [9,10].

CP585, *Rarefied Gas Dynamics: 22nd International Symposium*, edited by T. J. Bartel and M. A. Gallis

Report Documentation Page

Report Date	Report Type	Dates Covered (from... to)
09JUL2000	N/A	-

Title and Subtitle One-way Flow of a Rarefied Gas Induced in a Circular Pipe with a Periodic Temperature Distribution	**Contract Number**
	Grant Number
	Program Element Number
Author(s)	**Project Number**
	Task Number
	Work Unit Number
Performing Organization Name(s) and Address(es) Department of Aeronautics and Astronautics, Graduate School of Engineering, Kyoto University, Kyoto 606-8501, Japan	**Performing Organization Report Number**
Sponsoring/Monitoring Agency Name(s) and Address(es) AOARD Unit 45002 APO AP 96337-5002	**Sponsor/Monitor's Acronym(s)**
	Sponsor/Monitor's Report Number(s)

Distribution/Availability Statement
Approved for public release, distribution unlimited

Supplementary Notes
Papers from Rarefied Gas Dynamics (RGD) 22nd International Symposium held in Sydney, Australia on 9-14 July 2000. See also ADM001341 for whole conference on cd-rom.

Abstract

Subject Terms

Report Classification unclassified	**Classification of this page** unclassified
Classification of Abstract unclassified	**Limitation of Abstract** UU

Number of Pages
8

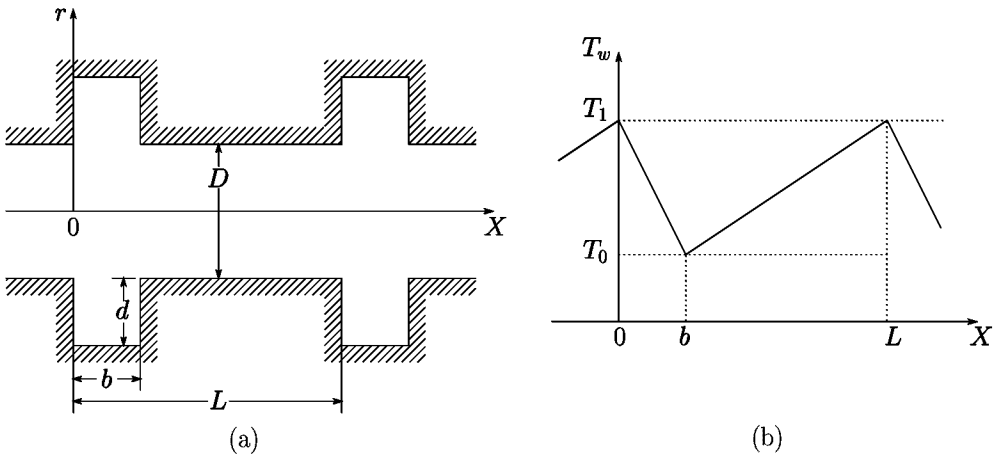

FIGURE 1. Pipe configuration and temperature distribution of the pipe wall.

PROBLEMS

We investigate the following two problems.

Problem I: Consider a rarefied gas in an infinitely long circular pipe with diameter D. A series of ring-shaped ditches with depth d and width b is dug periodically with period L, as shown in Fig. 1(a), where $(r,\ \theta,\ X)$ is a cylindrical coordinate system with X axis along the axis of the pipe. The pipe wall is kept at temperature T_w with a piecewise linear and periodic distribution with period L as shown in Fig. 1(b) (the minimum and maximum temperatures are T_0 and T_1, respectively). The gas molecules are assumed to be hard spheres and make the diffuse reflection on the pipe wall. Assuming that the flow field is axisymmetric and periodic in X, investigate the steady flow induced in the pipe for a wide range of the Knudsen number on the basis of kinetic theory. The periodic condition means that no pressure gradient is imposed externally.

Problem II: As shown below, a one-way flow is induced in Problem I. To investigate its pumping effect, consider the case where the pipe in Problem I is closed at $X = 0$ and $\mathcal{N}L$ ($\mathcal{N}$: positive integer) by diffusely reflecting walls with temperature T_1 and investigate the pressure distribution in the pipe.

RESULTS OF COMPUTATION AND DISCUSSIONS

Since the DSMC scheme adopted here is essentially the same as that explained in [1], we omit it for shortness and give only the result. The following notation is used in this paper: p is the pressure, T the temperature, v_r, v_θ $(= 0)$, and v_X the r, θ, and X components of the flow velocity, ρ_{av} the average density over a period (Problem I) or the entire pipe (Problem II), l_0 the mean free path of the gas molecules in the equilibrium state at rest with density ρ_{av}, i.e., $l_0 = m/\sqrt{2}\pi d_m^2 \rho_{av}$ with m and d_m being the mass and diameter of a molecule, Kn$= l_0/D$ the Knudsen number, $\mathcal{M}$ the mass flow in the X direction per unit time and per unit cross-sectional area of the part without ditches ($\pi D^2 \mathcal{M}/4$: the mass-flow rate through the pipe), and R the specific gas constant.

One-way flow

We first give the result for Problem I in the cases $T_1/T_0 = 3$, $L/D = 2$, $b/D = 1/2$ and various d/D, i.e., $d/D = 1/2$ (Case 1), 1/4 (Case 2), 1/8 (Case 3), 1 (Case 4), and 0 (Case 5).

Figure 2 shows some results of Case 1 (a given geometrical configuration) for different Knudsen numbers: the flow velocity vector $(v_X,\ v_r)$ and the isothermal lines for Kn$= 0.05$, 0.5, and 2 are shown in Figs. 2(a)–2(c) (note the difference of the scale of the arrow), and the dimensionless mass-flow rate $\mathcal{M}/\rho_{av}(2RT_0)^{1/2}$ versus Kn is

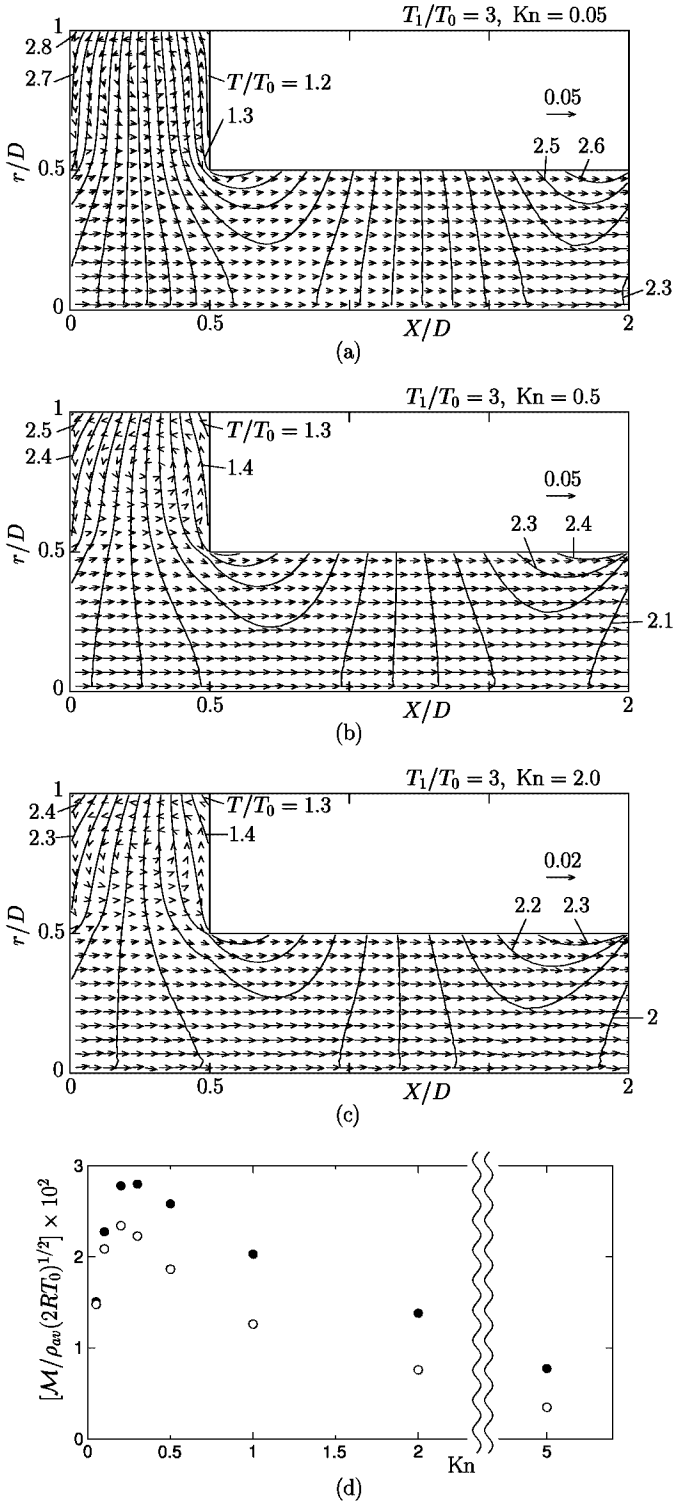

FIGURE 2. Induced one-way flow and mass-flow rate for $T_1/T_0 = 3$, $L/D = 2$, $b/D = 1/2$, and $d/D = 1/2$ (Case 1). (a) Kn = 0.05, (b) Kn = 0.5, (c) Kn = 0.2, (d) mass-flow rate $\mathcal{M}$ vs Kn. In (a)–(c), the arrow indicates the flow velocity vector (v_X, v_r) at its starting point; the scale of $(v_X^2 + v_r^2)^{1/2}/(2RT_0)^{1/2} = 0.05$ [(a), (b)] or 0.02 [(c)] is shown in the figures. The solid line indicates an isothermal line; the difference of T/T_0 between neighboring lines is 0.1. In (d), ○ indicates the present result, and • the result for the two-dimensional channel (cf. Fig. 5 in [1]).

shown in Fig. 2(d). The numerical value of $\mathcal{M}/\rho_{av}(2RT_0)^{1/2}$ is given in Table 1. In Fig. 2(d), the corresponding result for the two-dimensional channel [i.e., $M/\rho_{av}(2RT_0)^{1/2}D$ in [1] (Case 1 and $T_1/T_0 = 3$); see Fig. 5 of [1]] is also shown for comparison. A one-way flow is induced in the direction of the temperature gradient of the non-ditch part of the pipe wall, and the maximum mass-flow rate is attained at around Kn = 0.2. The flow vanishes in the free molecular gas (Kn=∞) [11] as well as in the continuum limit (Kn=0_+). The mass-flow rate per unit area is smaller in the case of a circular pipe.

In Fig. 3, the flow velocity vector and the isothermal lines at Kn = 0.5 are shown for various depths of the ditches, i.e., for Cases 2–5. The mass-flow rate in these cases is given in Table 2. When there is no ditch (Case 5), the one-way flow vanishes (more precisely, the mass-flow rate becomes a small quantity of the order of the error of the numerical computation). However, even the ditches with small depth cause an appreciable one-way flow (Case 3). The mass-flow rate does not depend much on the depth of the ditches for $d/D \geq 1/4$. These situations are qualitatively similar to those for the two-dimensional channel [1].

The data for the present DSMC computation is as follows. The initial distribution is the stationary Maxwellian with density ρ_{av} and temperature T_0. The gas region in the Xr plane ($0 \leq X \leq L$) is divided into uniform square cells of size $D/80 \times D/80$, and the total number of simulation particles is 100×(number of cells) (e.g., 8×10^5 in Case 1). The time step Δt is $2t_0/\sqrt{\pi}\times10^{-2}$ for Kn≤0.5 and $t_0/\sqrt{\pi}$Kn $\times10^{-2}$ for Kn> 0.5, where $t_0=(\sqrt{\pi}/2)(2RT_0)^{-1/2}l_0$ is the mean free time corresponding to l_0. The result shown above is the average over more than $2\times10^6\Delta t$ (Kn=0.05), $10^6\Delta t$ (Kn=0.1), $5\times10^5\Delta t$ (Kn=0.2), $4\times10^5\Delta t$ (Kn=0.3), or $3\times10^5\Delta t$ (other Kn) after the steady state is judged to have been established. For Case 1, a computation with coarser cells [square cells of size $D/40\times D/40$, 100×(number of cells) particles in total] was also carried out, and it was confirmed that the flow velocity vector and the isothermal lines agree fairly well with those by $D/80\times D/80$ system. The mass-flow rate obtained by the use of $D/40\times D/40$ system is shown in the parentheses in Table 1.

Although the total mass flow across the cross section at X per unit time is independent of X theoretically, its numerical result varies with X because of numerical error. The variation provides a good measure for accuracy. The relative difference between the maximum and the minimum is 0.5% or smaller, 1% or smaller, and 2.5% or smaller, respectively, in the cases where $[\mathcal{M}/\rho_{av}(2RT_0)^{1/2}]\times10^2$ is larger than 1.5, larger than 0.5, and smaller than 0.5 (except Case 5) for $D/80\times D/80$ system. Another measure of accuracy is the θ component v_θ of the flow velocity, i.e., it should vanish theoretically but takes nonzero values in the DSMC computation. For example, $|v_\theta|/(2RT_0)^{1/2}$ is smaller than 6.60×10^{-4} (Kn=0.05), 5.93×10^{-4} (Kn=0.2), 4.03×10^{-4} (Kn=0.5), and 4.43×10^{-4} (Kn=2) in 80% of the cells in Case 1 [the maximum speed v_{max} in the corresponding cases is: $v_{max}/(2RT_0)^{1/2}=3.07\times10^{-2}$, 4.45×10^{-2}, 3.11×10^{-2}, and 1.31×10^{-2}, respectively] for $D/80\times D/80$ system.

TABLE 1. Mass-flow rate $\mathcal{M}$ versus Knudsen number for $T_1/T_0 = 3$, $L/D = 2$, $b/D = 1/2$, and $d/D = 1/2$ (Case 1). The value in the parentheses is the result obtained by the use of a coarser cell system (see the second paragraph from the last in this subsection).

Kn	$\mathcal{M}/\rho_{av}(2RT_0)^{1/2}$		Kn	$\mathcal{M}/\rho_{av}(2RT_0)^{1/2}$	
0.05	1.476×10^{-2}	(1.427×10^{-2})	0.5	1.863×10^{-2}	(1.860×10^{-2})
0.1	2.083×10^{-2}	(2.060×10^{-2})	1	1.262×10^{-2}	(1.249×10^{-2})
0.2	2.345×10^{-2}	(2.326×10^{-2})	2	7.593×10^{-3}	(7.591×10^{-3})
0.3	2.225×10^{-2}	(2.234×10^{-2})	5	3.482×10^{-3}	(3.491×10^{-3})

TABLE 2. Mass-flow rate $\mathcal{M}$ at Kn = 0.5 for various depths of the ditches in the case $T_1/T_0 = 3$, $L/D = 2$, and $b/D = 1/2$.

d/D	0 (Case 5)	1/8 (Case 3)	1/4 (Case 2)	1/2 (Case 1)	1 (Case 4)
$\mathcal{M}/\rho_{av}(2RT_0)^{1/2}$	6.790×10^{-5}	1.040×10^{-2}	1.506×10^{-2}	1.863×10^{-2}	1.921×10^{-2}

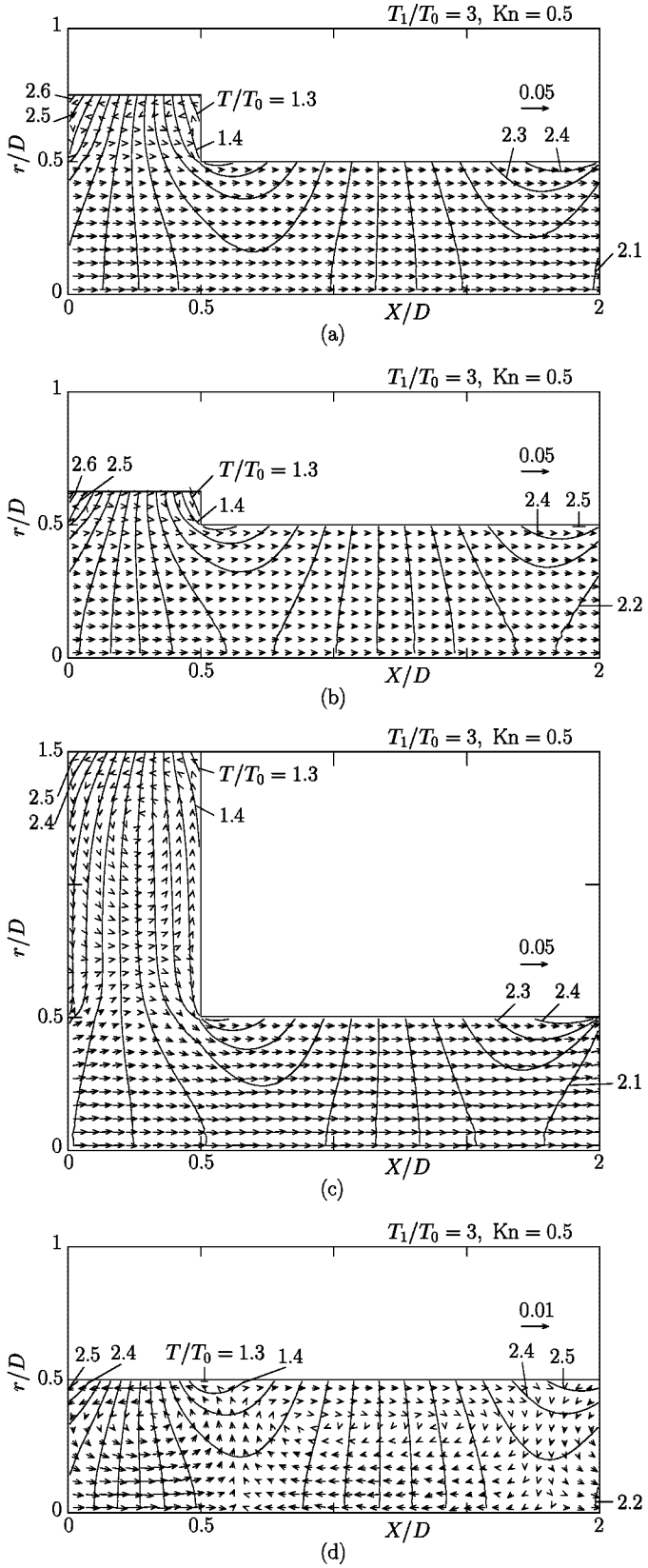

FIGURE 3. Induced one-way flow at Kn = 0.5 for various depths of the ditches in the case $T_1/T_0 = 3$, $L/D = 2$, and $b/D = 1/2$. (a) $d/D = 1/4$ (Case 2), (b) $d/D = 1/8$ (Case 3), (c) $d/D = 1$ (Case 4), (d) $d/D = 0$ (Case 5). See the caption of Fig. 2. The scale of $(v_X^2 + v_r^2)^{1/2}/(2RT_0)^{1/2} = 0.05$ [(a)–(c)] or 0.01 [(d)] is shown in the figures.

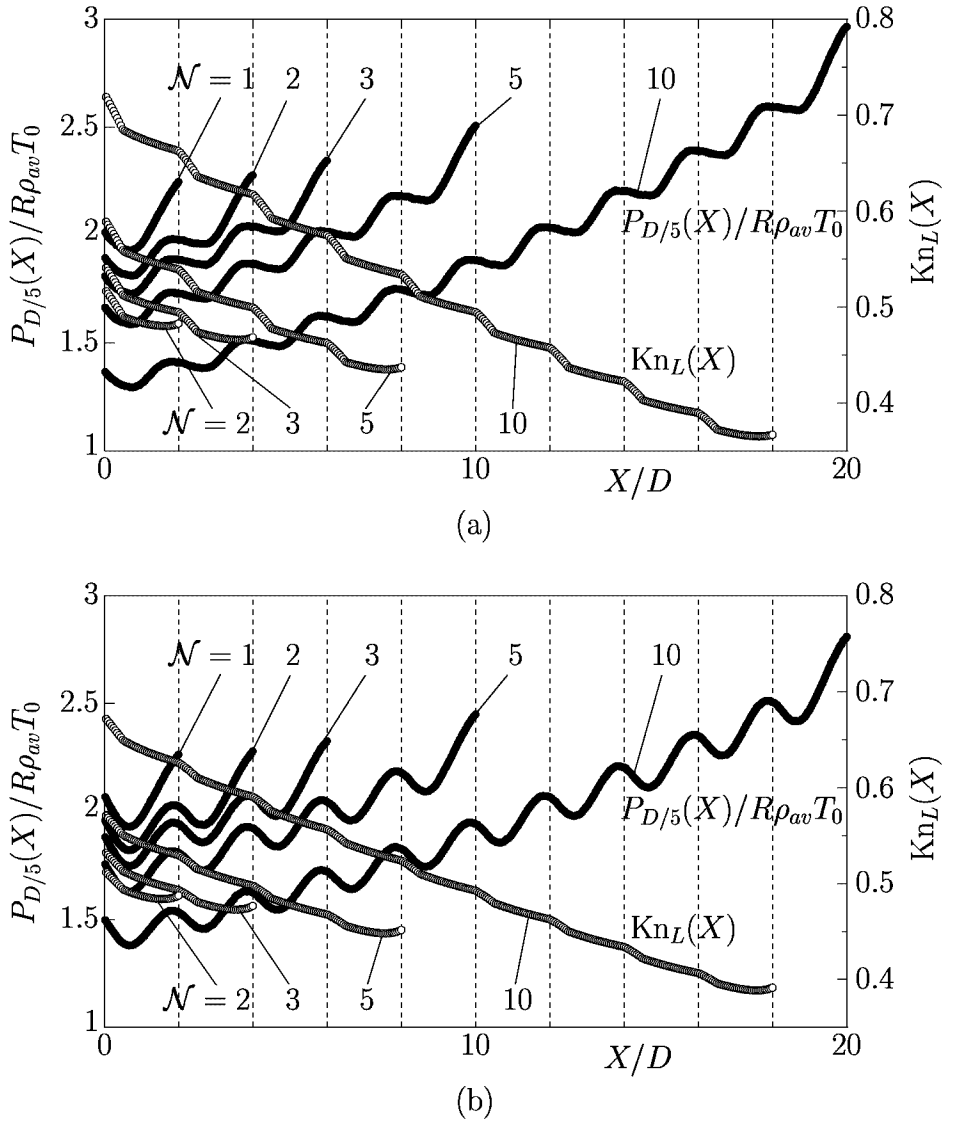

FIGURE 4. The distributions of $P_{D/5}(X)$ and $\mathrm{Kn}_L(X)$ in the closed pipe with various $\mathcal{N}$ for $T_1/T_0 = 3$, $L/D = 2$, $b/D = 1/2$, and $\mathrm{Kn} = 0.5$. (a) the case corresponding to Case 1 ($d/D = 1/2$), (b) the case corresponding to Case 2 ($d/D = 1/4$).

Pumping effect

We next investigate Problem II in the case $T_1/T_0 = 3$, $L/D = 2$, and $b/D = 1/2$. To begin with, we define the average pressure $P_a(X)$ near the center of the cross section at X by $P_a(X)=2(2/a)^2 \int_0^{a/2} p(r, X)rdr$ and a semi-local Knudsen number $\mathrm{Kn}_L(X)$ by $l_L(X)/D$, where $l_L(X)$ is the mean free path of the gas molecules in the equilibrium state at rest with density being the average density $\rho_{avL}(X)$ in the interval $[X,\ X + L]$, i.e., $l_L(X)=m/\sqrt{2}\pi d_m^2 \rho_{avL}(X)$. The $D/40\times D/40$ system is used for the computation of the present problem.

Figure 4 shows the distributions of $P_{D/5}(X)$ and $\mathrm{Kn}_L(X)$ for $\mathrm{Kn} = 0.5$ and $\mathcal{N}$=1, 2, 3, 5, and 10 in the cases corresponding to Case 1 ($d/D = 1/2$) and Case 2 ($d/D = 1/4$) in Problem I. The pressure rise over ten periods is about 117% in Fig. 4(a) and about 88% in Fig. 4(b), whereas it is about 60% for the two-dimensional channel corresponding to the case of Fig. 4(a) (see Fig. 11 of [1]). Although the induced one-way flow is stronger in the two-dimensional channel system, the pressure rise is larger (or the pumping effect is stronger) in the pipe

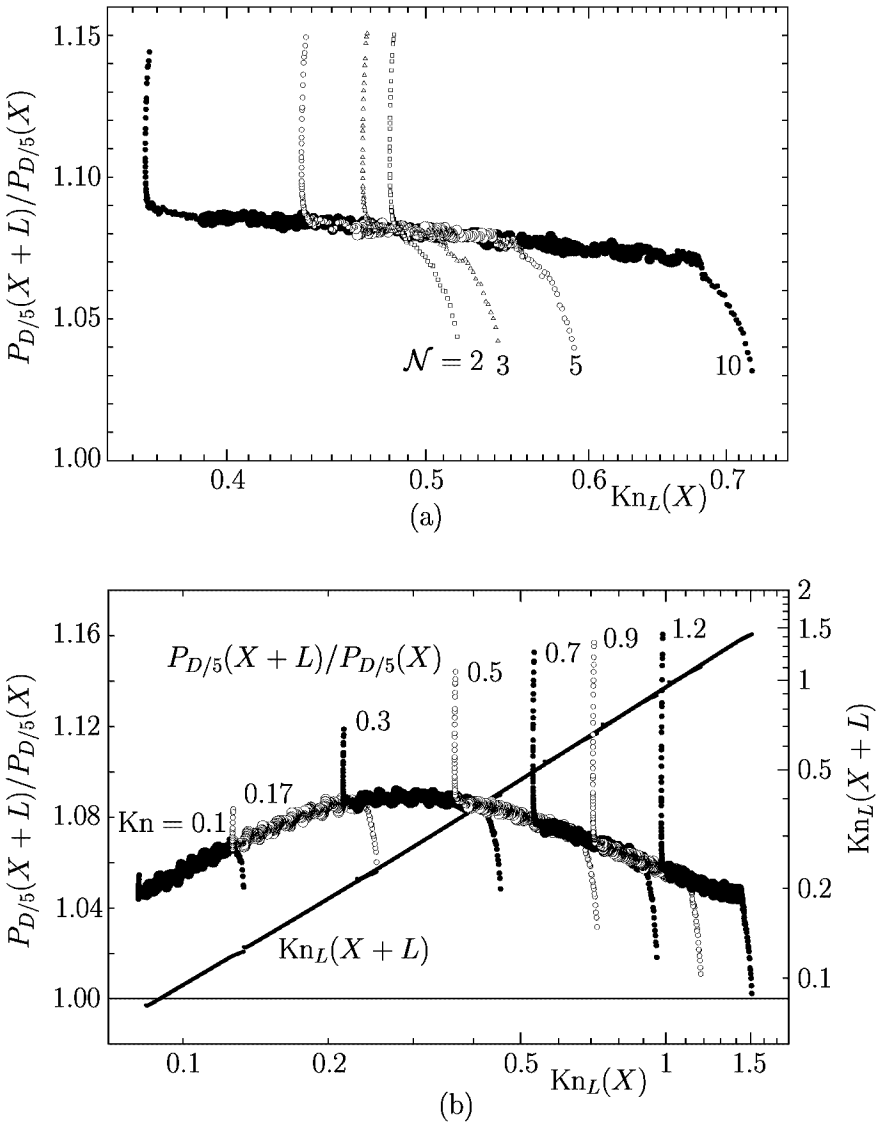

FIGURE 5. $P_{D/5}(X+L)/P_{D/5}(X)$ and $\mathrm{Kn}_L(X+L)$ vs $\mathrm{Kn}_L(X)$ for the closed pipe in the case $T_1/T_0 = 3$, $L/D = 2$, $b/D = 1/2$, and $d/D = 1/2$ (the case corresponding to Case 1). (a) $\mathcal{N} = 2$, 3, 5, and 10 and $\mathrm{Kn} = 0.5$, (b) $\mathcal{N} = 10$ and various Kn. The data in the middle region $[L \le X \le (\mathcal{N}-2)L]$ are shown by larger symbols, and those in the end regions $[0 \le X < L$ and $(\mathcal{N}-2)L < X \le (\mathcal{N}-1)L]$ by smaller symbols.

system.

For a given set of the parameters (L/D, d/D, b/D, T_1/T_0, Kn, $\mathcal{N}$), the pressure ratio $P_{D/5}(X+L)/P_{D/5}(X)$ can be expressed as a function of $\mathrm{Kn}_L(X)$ because $\mathrm{Kn}_L(X)$ is monotonic in X. Figure 5(a) shows the former versus the latter for $\mathcal{N}$=2, 3, 5, and 10 in the case of $d/D = 1/2$ and $\mathrm{Kn} = 0.5$. The data in the middle region $[L \le X \le (\mathcal{N}-2)L]$ are shown by larger symbols, and those in the end regions $[0 \le X < L$ and $(\mathcal{N}-2)L < X \le (\mathcal{N}-1)L]$ by smaller symbols. The data with larger symbols lie on a single curve irrespective of $\mathcal{N}$. The data with smaller symbols away from the middle region project upward and downward sharply. The sharp projections are attributed to the end effect, and it is limited within the first and the last section. Taking into account this feature, we can obtain the curve $P_{D/5}(X+L)/P_{D/5}(X)$ versus $\mathrm{Kn}_L(X)$ for a wide range $\mathrm{Kn}_L(X)$, instead of the computation for large $\mathcal{N}$, by joining the pieces of the curve obtained for a fixed $\mathcal{N}$ (say $\mathcal{N} = 10$) and different Kn. By this computation, the result for large $\mathcal{N}$ can be obtained by

a smaller computer. Such an example is given in Fig. 5(b), where the curve for $d/D = 1/2$ is constructed by the data for seven different Kn (with $\mathcal{N} = 10$), i.e., Kn = 0.1, 0.17, 0.3, 0.5, 0.7, 0.9, and 1.2. As in [1], from this curve and the line of $\mathrm{Kn}_L(X + L)$ versus $\mathrm{Kn}_L(X)$ shown also in Fig. 5(b), one can estimate the maximum compression ratio attained when two reservoirs are joined by a pipe consisting of a large number (say $\mathcal{N}'$) of periods. Let $X = 0$ be the entrance of the low-pressure side and suppose that $P_{D/5}(0)$ and $\mathrm{Kn}_L(0)$ are approximately given by the pressure and the local Knudsen number there. Then, by reading $[P_{D/5}(L)/P_{D/5}(0), \mathrm{Kn}_L(L)]$, $[P_{D/5}(2L)/P_{D/5}(L), \mathrm{Kn}_L(2L)]$, ..., $[P_{D/5}(\mathcal{N}'L)/P_{D/5}((\mathcal{N}' - 1)L), \mathrm{Kn}_L(\mathcal{N}'L)]$ successively from the figure, we can obtain the total compression ratio $P_{D/5}(\mathcal{N}'L)/P_{D/5}(0)$, which is the approximate compression ratio between the reservoirs. For example, a pipe system consisting of forty periods gives compression ratio about 15 when $\mathrm{Kn}_L(0) = 1 \sim 1.5$. This is three times larger than compression ratio about 5 attained by the corresponding two-dimensional channel system [1].

REFERENCES

1. Sone, Y., Waniguchi, Y., and Aoki, K., *Phys. Fluids* **8**, 2227 (1996).
2. Bird, G. A., *Molecular Gas Dynamics*, Oxford: Oxford Univ. Press, 1976.
3. Bird, G. A., *Molecular Gas Dynamics and the Direct Simulation of Gas Flows*, Oxford: Oxford Univ. Press, 1994.
4. Knudsen, M., Ann. Phys. **31**, 205 (1910); **33**, 1435 (1910).
5. Kennard, E. H., *Kinetic Theory of Gases*, New York: McGraw-Hill, 1938, p. 327.
6. Sone, Y., and Yamamoto, K., *Phys. Fluids* **11**, 1672 (1968); Errata: *Phys. Fluids* **13**, 1651 (1970).
7. Ohwada, T., Sone, Y., and Aoki, K., *Phys. Fluids A* **1**, 2042 (1989).
8. Sone, Y., *Annual Rev. Fluid Mech.* **32**, 779 (2000).
9. Sone, Y., and Sato, K., *Phys. Fluids* **12**, 1864 (2000).
10. Sone, Y., Fukuda, T., Hokazono, T., and Sugimoto, H., This symposium.
11. Sone, Y., *J. Méc. Théor. Appl.* **3**, 315 (1984); **4**, 1 (1985).